DALTON
FULL PAPER

Bis(R-bipyridyl)ruthenium bibenzimidazole complexes (R = H, Me or Bu^t): supramolecular arrangement *via* hydrogen bonds, photo- and electro-chemical properties and reactivity towards carbon dioxide

Sven Rau,[a] Mario Ruben,[a] Torsten Büttner,[a] Christian Temme,[a] Sylvana Dautz,[a] Helmar Görls,[a] Manfred Rudolph,[a] Dirk Walther,*[a] Andre Brodkorb,[b] Marco Duati,[c] Christine O'Connor[c] and Johannes G. Vos*[c]

[a] *Institut für Anorganische und Analytische Chemie, Friedrich-Schiller-University, 07743 Jena, Germany*
[b] *Laboratoire de Chimie Organique Physique, CP 160/80, Université Libre de Bruxelles, 1050 Bruxelles, Belgium*
[c] *Inorganic Chemistry Research Centre, School of Chemical Sciences, Dublin City University, Dublin 9, Ireland*

Received 18th May 2000, Accepted 24th August 2000
First published as an Advance Article on the web 28th September 2000

Complexes of the type $[Ru(H_2bibzim)(R\text{-}bpy)_2X_2\cdot nH_2O$ (R = H, 2,2′-bipyridine, bpy, X = $CF_3SO_3^-$ **1**; R = Me, 4,4′-dimethyl-2,2′-bipyridine, dmbpy, X = PF_6^- **2**; R = *tert*-butyl, 4,4′-di-*tert*-butyl-2,2′-bipyridine, tbbpy, X = Cl^- **3**; H_2bibzim = 1,1′-bibenzimidazole) containing two NH functions acting as hydrogen bond donors formed different spatially highly organised supramolecular assemblies with water. X-Ray investigation revealed that the nature of the counter ion influences the hydrogen bonding pattern and extent of spatial organisation. In **2** one dimensional chains of hydrogen bonded water could be found. In the deprotonated complex $[Ru(bibzim)(tbbpy)_2]$ **4** water molecules serve as hydrogen bond donors. The diastereomeric forms **5a/5b** of the homodinuclear ruthenium complex $[\{Ru(tbbpy)_2\}_2(bibzim)][PF_6]_2$ could be separated. No differences in their photophysical properties could be detected. The X-ray investigation of **5a** and $[\{Ru(bpy)_2\}_2(bibzim)][PF_6]_2$ **6** showed little influence of peripheral substitution on structural properties. Complexes **3**–**5** exhibit activity in electrochemical CO_2 reduction which can be tuned by variation of the degree of protonation of the bibenzimidazole.

Introduction

The chemistry of polypyridine ruthenium(II) complexes bridged by bi- or tri-dentate ligands[1] has received much attention in connection with the construction of molecular electronic devices.[2] Suitable bridging ligands are for example bipyrimidine,[3] substituted pyrazines,[4] substituted bipyridines[5] and biimidazoles.[6] In the last few years ruthenium polypyridyl complexes based on benzimidazole moieties have been investigated in detail.[7] These studies have concentrated on the spectroscopic and electrochemical properties of these complexes. The presence of the acidic imidazole proton allows deprotonation of the complexes and this results in a rich chemistry where changes in pH can be used to determine the electrochemical and photophysical properties of the compounds.[8] This, deprotonation of bibenzimidazole for instance allows for the formation of di- and oligo-nuclear complexes.[9] Additionally, ruthenium benzimidazole complexes can be used as catalysts for the electrochemical reduction of CO_2[10] and their application as proton driven molecular switches has been reported.[11] Recently we have found that a substituted, deprotonated bibenzimidazole can act as a metal sensor.[12]

Considering the large number of studies carried out on ruthenium compounds in solution it is surprising that there has been much less interest in the study of these compounds in well defined solid state environments.[13–15] The presence of the imidazole nitrogen atoms in benzimidazole complexes in both their protonated and deprotonated state should be an ideal building block for the construction of solid state supramolecular structures based on hydrogen bonding. Our interest in these compounds is twofold. First we would like to use the imidazole unit as a building block for the construction of well defined solid state structures. Secondly we are interested to see whether the known dependence of photophysical properties on the stereochemistry of ruthenium complexes[16] is also valid for bibenzimidazole based systems.

In this contribution we report on a number of syntheses and crystal structures of benzimidazole containing ruthenium polypyridyl complexes. The structures obtained show some well defined hydrogen bonding patterns. We also show that the separation of the stereoisomers of the homodinuclear complexes is possible and that the photophysical properties of these isomers are independent of their stereochemistry. In addition we report on the catalytic properties of these compounds for the electrochemical reduction of CO_2. All compounds obtained are fully characterized by X-ray crystallography, NMR, UV-vis and emission spectroscopy.

Experimental

Materials

All synthetic work was performed using Schlenk techniques. Emission and absorption spectra were recorded using septum equipped luminescent cells (Hellma) in spectroscopic acetonitrile (Fluka) and THF (Aldrich). THF was dried and distilled over sodium–benzophenone, CH_3CN was dried over CaH_2 and distilled; all other solvents were distilled prior to use.

DOI: 10.1039/b003992f

$[Ru(COD)Cl_2]_n$,[17] bibenzimidazole (H_2bibzim),[18] 4,4′-di-*tert*-butyl-2,2′-bipyridine (tbbpy),[19] $Ru(bpy)_2Cl_2$,[20] $Ru(dmbpy)_2Cl_2$ (dmbpy = 4,4′-dimethyl-2,2′-bipyridine),[21] [Ru(bibzim)(tbbpy)$_2$][12] and [{Ru(bpy)$_2$}$_2$(bibzim)][PF_6]$_2$[7] were synthesized using literature methods. Oxalic acid and NH_4ClO_4 (Fluka) were used without further purification.

Preparations

[Ru(tbbpy)$_2$Cl$_2$]. 12.08 g (0.043 mol) $[Ru(COD)Cl_2]_n$ and 23.2 g (0.086 mol) tbbpy were refluxed in 40 cm^3 DMF for 72 h. The DMF and cycloocta-1,5-diene were removed by vacuum distillation and the resulting black microcrystalline compound was dried under vacuum for 2 h. The complex was purified by Soxhlet extraction with toluene. The toluene was removed and the resulting dark microcrystalline compound dried under vacuum for 3 h. Yield: 78%. ^{1}H NMR (acetone-d_6): δ 10.02 (1 H, d, H6), 8.54 (1 H, s, H3), 8.42 (1 H, s, H3a), 7.68 (1 H, d, H5), 7.48 (1 H, d, H6a), 7.08 (1 H, d, H5a), 1.51 (9 H, s, t-butyl) and 1.31 (9 H, s, t-butyl). UV (THF) λ_{max} = 583 nm. MS: *m*/*z* = 708 (corresponding isotope pattern for $C_{36}H_{48}N_4Cl_2Ru$).

[Ru(H$_2$bibzim)(R-bpy)$_2$]X$_2$ 1–3. These were synthesized using standard procedures.[7,9] **CAUTION**: perchlorates are potentially explosive. After removal of the solvent 10 cm^3 water were added followed by a concentrated aqueous solution of NH_4PF_6, $LiCF_3SO_3$ or $LiClO_4$ respectively. If no counter ion source was added the complex was obtained as its dichloride and purified using the same techniques. The resulting precipitate was filtered off, redissolved in acetonitrile, filtered and then the solvent was removed. Yields were above 90% for all compounds. ES-MS: [Ru(H$_2$bibzim)(bpy)$_2$][PF_6]$_2$ **1**, *m*/*z* = 647 (corresponding isotope pattern for $C_{34}H_{25}N_8Ru$); [Ru(H$_2$bibzim)(dmbpy)$_2$][PF_6]$_2$ **2**, *m*/*z* = 702 (corresponding isotope pattern for $C_{38}H_{33}N_8Ru$); [Ru(H$_2$bibzim)(tbbpy)$_2$][PF_6]$_2$ **3**, *m*/*z* = 871 (corresponding isotope pattern for $C_{50}H_{57}N_8Ru$). The compounds were also characterized using ^{1}H NMR (Table 2), UV-vis and emission (Table 3) and cyclic voltammetry (Table 3). Suitable crystals for X-ray crystallography were obtained by slow evaporation of an acetone–water solution (1 : 1) of **1** and **2** and of an acetonitrile–water solution (1 : 1) of **3**.

[Ru(bibzim)(tbbpy)$_2$] 4. This was recrystallized from an acetone–water (50 : 50) solution as the dihydrate.

[{Ru(tbbpy)$_2$}$_2$(bibzim)][PF_6]$_2$ 5. This was synthesized using 369 mg of [Ru(tbbpy)$_2$Cl$_2$] (0.52 mmol) and 61 mg (0.26 mmol) H_2bibzim refluxed with 2 cm^3 triethylamine for 20 h in 100 cm^3 ethanol–water (1 : 1). The solution was allowed to cool, filtered and the solvent removed. The dark residue was redissolved in 10 cm^3 of water. A concentrated aqueous solution of NH_4PF_6 was added. The resulting precipitate was filtered off and redissolved in 100 cm^3 acetone–water (1 : 1) and left to recrystallize. The precipitate was filtered off and analysed by ^{1}H NMR spectroscopy. Two isomers could be identified. The precipitate was purified by recrystallization and two pure fractions of the complex could be separated. Alternatively [Ru(bibzim)(tbbpy)$_2$] can be refluxed with one equivalent of [Ru(tbbpy)$_2$Cl$_2$] in ethanol–water (1 : 1) for 8 h and the resulting compound treated in the same way as described for the former synthesis. Yield for both methods: 0.25 mmol (96%). After obtaining the pure fractions recrystallization from acetone water (50 : 50) yielded suitable crystals for X-ray diffraction for the *meso* isomer **5a**. ^{1}H NMR, see Table 2. UV-vis, electrochemical data and emission, see Table 3.

[{Ru(bpy)$_2$}$_2$(bibzim)][PF_6]$_2$ 6. This was crystallized by slow evaporation of an acetonitrile–water solution (50 : 50) of the diastereomeric mixture.

Instrumentation

NMR spectra were recorded using Bruker 400 and 200 MHz spectrometers, UV-VIS spectra using a Varian Cary 1 UV-vis or a Shimadzu UV 3100 UV-vis-NIR spectrometer. Emission spectra are not corrected and were recorded using a Perkin-Elmer LS50B spectrometer equipped with a Hamamatsu R928 red sensitive detector. IR spectra were recorded using a Perkin-Elmer 2000 FT-IR spectrometer.

Lifetime measurements

Luminescent lifetimes were measured employing a Spectra Physics Nd-YAG frequency tripled, Q-switched laser as excitation source coupled in a right angled configuration to an Oriel iCCD; laser power was measured as 30 mJ per 20 ns pulse. The single photon counting (SPC) measurements for the dinuclear complexes were performed with an Edinburgh Instruments FL-900 spectrofluorimeter equipped with a nitrogen filled discharge lamp and a Peltier-cooled Hamamatsu R-928 PM tube. The emission decays were analysed with the Edinburgh Instruments software (version 3.0), based on non-linear least squares regression using a modified Marquardt algorithm.

Electrochemical equipment

The cyclic voltammetric measurements were made with a home built computer controlled instrument based on the DAP-3200a data acquisition board (DATALOG Systems) as well as with the Autolab PG Stat 20 (Metrohm). The experiments were performed in a three electrode cell under a blanket of solvent saturated argon or carbon dioxide respectively. The ohmic resistance which had to be compensated for was obtained by measuring the impedance of the system at potentials where the faradaic current was negligibly small. Background correction was accomplished by subtracting the current curves of the blank electrolyte (containing the same concentration of supporting electrolyte) from the experimental curve. The reference was an Ag–AgCl electrode in acetonitrile containing 0.25 M tetra-n-butylammonium chloride but for convenience all potentials were finally referenced to the SCE[22] throughout. Exhaustive electrolyses of complexes were performed with 0.001 M solutions of the complexes in dried acetonitrile with 1 M tetra-n-butylammonium perchlorate as supporting electrolyte using a Bank potentiostat. Solvent and mercury were removed and the complex resuspended in 2 cm^3 water followed by extraction with 2 cm^3 $CHCl_3$. Oxalate was determined in the aqueous phase. The yield of oxalate was determined using a Knauer HPLC system with a C_{18} column and 5% H_3PO_4 as mobile phase, equipped with a Knauer absorbance detector UV-1 set at 208 nm calibrated with a solution of oxalic acid. Oxalic acid was additionally identified by subtracting IR spectra of the complex in solution before and after the electrolysis where the band at 1645 cm^{-1} was assigned to oxalic acid.

Mass spectroscopy

The mass spectra were recorded using a SSQ 170, Finnigan MAT, electrospray mass spectra on a Finnigan MAT, MAT 95 XL instrument. In the ESI process the sample used for the photochemical investigation (*ca.* 10^{-5} M solution in THF) was introduced into the ESI ion source with a Harvard Apparatus syringe infusion pump, Model 22, with a flow rate of 5–20 l min^{-1}. The positive ES mass spectra were obtained with voltages of 3–4 kV applied to the electrospray needle. The resolution was usually about 2000 at *m*/*z* 750.

Crystal structure determination

The intensity data for the compounds were collected on a Nonius KappaCCD diffractometer, using graphite-monochrom-

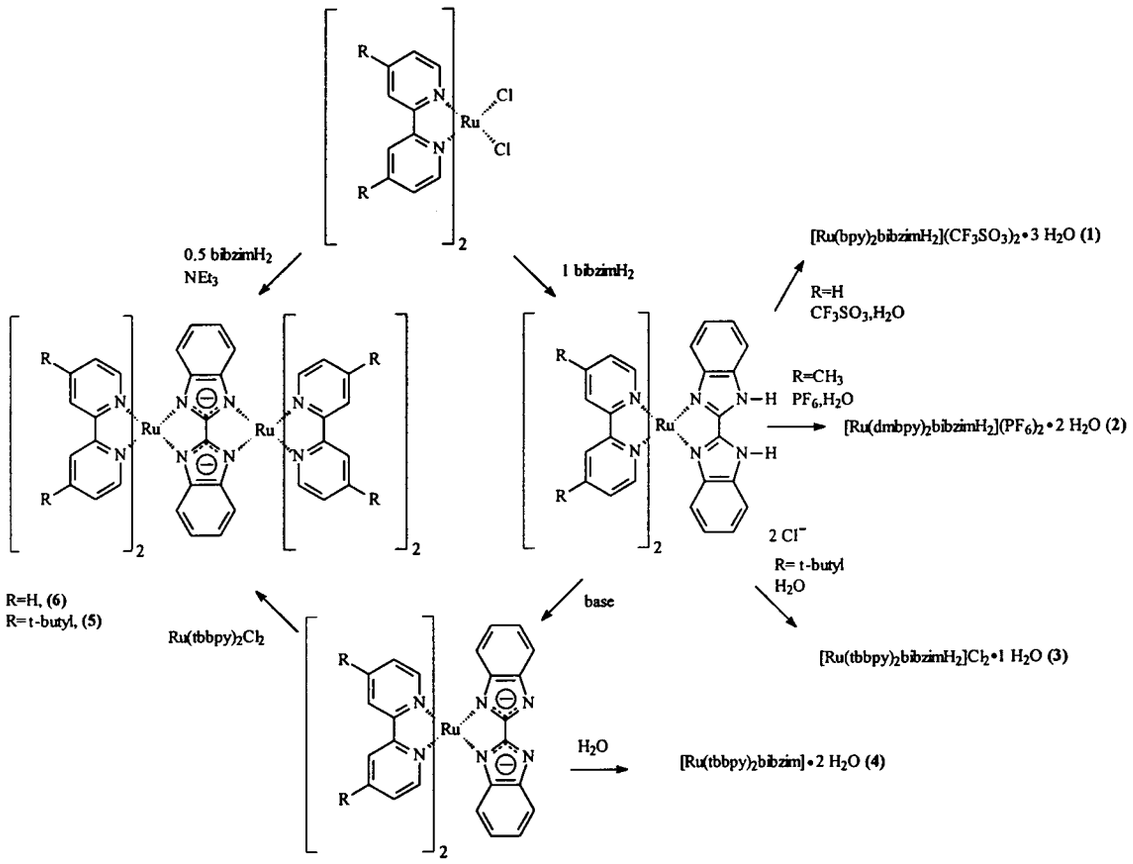

Scheme 1 Synthesis of the complexes **1**–**6**.

ated Mo-Kα radiation. Data were corrected for Lorentz and polarization effects, but not for absorption.[23] The structures were solved by direct methods (SHELXS[24]) and refined by full-matrix least squares techniques against F_o^2 (SHELXL 97[25]). For the compound **2** the hydrogen atoms of the "amine group" and the water molecules were located by Fourier difference synthesis and refined isotropically. All other hydrogen atoms were included at calculated positions with fixed thermal parameters. All non-hydrogen atoms were refined anisotropically.[25] XP (Siemens Analytical X-Ray Instruments, Inc.) was used for structure representations.

Crystal data. $[Ru(H_2bibzim)(bpy)_2][CF_3SO_3]_2\cdot 3H_2O$ **1**. $C_{36}H_{26}F_6N_8O_6RuS_2$, $M_r = 999.34$ g mol^{-1}, monoclinic, space group $C2/c$, $a = 22.0290(10)$, $b = 16.2900(10)$, $c = 13.3542(6)$ Å, $\beta = 122.214(2)°$, $V = 4054.5(4)$ Å^3, $T = -90$ °C, $Z = 4$, μ(Mo-Kα) = 5.81 cm^{-1}, 20269 reflections measured, 4590 independent reflections, $R_{int} = 0.101$, 3531 reflections with $F_o > 4\sigma(F_o)$, $R1_{obs} = 0.095$, $wR2_{obs} = 0.222$, $R1_{all} = 0.128$, $wR2_{all} = 0.241$.

$[Ru(H_2bibzim)(dmbpy)_2][PF_6]_2\cdot 2H_2O\cdot 2C_3H_6O$ **2**. $C_{38}H_{34}F_{12}N_8P_2Ru\cdot 2C_3H_6O\cdot 2H_2O$, $M_r = 1145.93$ g mol^{-1}, monoclinic, space group $C2/c$, $a = 22.7551(5)$, $b = 23.9120(5)$, $c = 9.6410(3)$ Å, $\beta = 112.708(3)°$, $V = 4839.2(2)$ Å^3, $T = -90$ °C, $Z = 4$, μ(Mo-Kα) = 4.88 cm^{-1}, 6467 reflections measured, 3362 independent, $R_{int} = 0.018$, 3075 with $F_o > 4\sigma(F_o)$, $R1_{obs} = 0.042$, $wR2_{obs} = 0.123$, $R1_{all} = 0.0467$, $wR2_{all} = 0.133$.

$[Ru(H_2bibzim)(tbbpy)_2]Cl_2\cdot H_2O\cdot 2CH_3CN$ **3**. Described previously.[12]

$[Ru(bibzim)(tbbpy)_2]\cdot 2H_2O\cdot C_3H_6O$ **4**. $C_{50}H_{56}N_8Ru\cdot C_3H_6O\cdot 2H_2O$, $M_r = 964.21$ g mol^{-1}, monoclinic, space group $C2/c$, $a = 11.7219(5)$, $b = 17.5925(8)$, $c = 24.522(1)$ Å, $\beta = 101.083(3)°$, $V = 4962.6(4)$ Å^3, $T = -90$ °C, $Z = 4$, μ(Mo-Kα) = 3.66 cm^{-1}, 5809 reflections measured, 3209 independent, $R_{int} = 0.045$, 3082 with $F_o > 4\sigma(F_o)$, $R1_{obs} = 0.053$, $wR2_{obs} = 0.148$, $R1_{all} = 0.069$, $wR2_{all} = 0.174$.

$[\{Ru(tbbpy)_2\}_2(bibzim)][PF_6]_2\cdot 6C_3H_6O$ **5a**. $C_{86}H_{104}F_{12}N_{12}P_2Ru_2\cdot 6C_3H_6O$, $M_r = 2146.36$ g mol^{-1}, triclinic, space group $P\bar{1}$, $a = 12.3749(3)$, $b = 14.4512(4)$, $c = 16.6108(5)$ Å, $\alpha = 80.763(2)$, $\beta = 88.971(2)$, $\gamma = 75.717(2)°$, $V = 2840.7(1)$ Å^3, $T = -90$ °C, $Z = 1$, μ(Mo-Kα) = 3.67 cm^{-1}, 20676 reflections measured, 11432 independent, $R_{int} = 0.047$, 9084 with $F_o > 4\sigma(F_o)$, $R1_{obs} = 0.063$, $wR2_{obs} = 0.155$, $R1_{all} = 0.085$, $wR2_{all} = 0.168$.

$[\{Ru(bpy)_2\}_2(bibzim)][PF_6]_2\cdot 3C_2H_3N\cdot 2H_2O$ **6**. $C_{54}H_{40}F_{12}N_{12}P_2Ru_2\cdot 3CH_3CN\cdot 2H_2O$, $M_r = 1508.25$ g mol^{-1}, monoclinic, space group $C2/c$, $a = 24.474(2)$, $b = 13.921(1)$, $c = 19.433(1)$ Å, $\beta = 106.843(3)°$, $V = 6336.9(8)$ Å^3, $T = -90$ °C, $Z = 4$, μ(Mo-Kα) = 6.19 cm^{-1}, 8224 reflections measured, 4504 independent, $R_{int} = 0.045$, 3666 with $F_o > 4\sigma(F_o)$, $R1_{obs} = 0.048$, $wR2_{obs} = 0.125$, $R1_{all} = 0.0635$, $wR2_{all} = 0.141$.

CCDC reference number 186/2160.

See http://www.rsc.org/suppdata/dt/b0/b003992f/ for crystallographic files in .cif format.

Results and discussion

Synthesis of complexes 1–6

All complexes could be obtained *via* standard procedures starting from the corresponding precursor $[Ru(R\text{-}bpy)_2Cl_2]$ (Scheme 1).[7] The complexes with R = H and CH_3 were synthesized according to literature methods.[20,21] However, in our hands the synthesis of the *tert*-butyl substituted complex did not proceed along standard procedures with reproducible relatively high yields. Instead of $[Ru(tbbpy)_2Cl_2]$ large quantities of $[Ru(tbbpy)_3Cl_2]$ were obtained. For this reason we developed a new route which is based on separation of the reduction and complex formation into a two step synthesis. In the first step $RuCl_3(H_2O)_x$ was treated with cycloocta-1,5-diene to form the polymeric ruthenium(II) complex $RuCl_2(COD)_n$ in good yields.[17] Refluxing of the polymeric compound with tbbpy in DMF and subsequent purification by extraction in step 2 resulted in the pure complex.

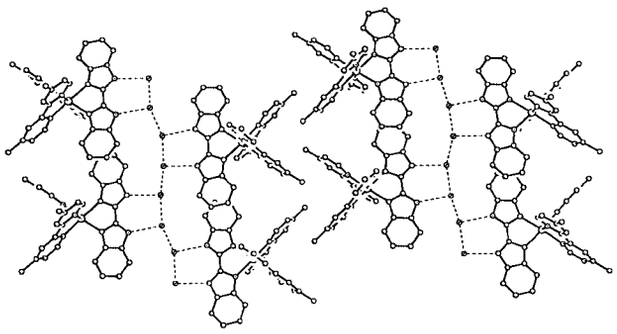

Fig. 1 Supramolecular arrangement of $[Ru(H_2bibzim)(dmbpy)_2]^{2+}$ **2** in the solid state; protons, anions and acetone molecules are omitted for clarity.

Complexation with bibenzimidazole yields the mono- or dinuclear compound depending on the molar ratio employed (Scheme 1). The dinuclear complex **5** was also accessible if the mononuclear complex was deprotonated, isolated and treated with one equivalent of $[Ru(tbbpy)_2Cl_2]$. Complexes **1**–**4** yield supramolecular structures characterized by different hydrogen bonding networks, synthesized according to Scheme 1.

Crystal structures of complexes 1–6

The complexes, $[Ru(bpy)_2(H_2bibzim)][CF_3SO_3]_2\cdot 3H_2O$ **1**, $[Ru(H_2bibzim)(dmbpy)_2][PF_6]_2\cdot 2H_2O$ **2**, $[Ru(H_2bibzim)(tbbpy)_2]Cl_2\cdot H_2O$[12] **3**, $[Ru(bibzim)(tbbpy)_2]\cdot 2H_2O$ **4**, *meso*-$[\{Ru(tbbpy)_2\}_2(bibzim)][PF_6]_2$ **5a** and *meso*-$[\{Ru(bpy)_2\}_2(bibzim)][PF_6]_2$ **6** could be obtained as single crystals suitable for X-ray investigation. Their solid state structures are displayed in Figs. 1–6. All investigated complexes possess a distorted octahedral co-ordination geometry at the ruthenium centre. The ruthenium–bipyridine distances are within the expected range and are within experimental errors invariant towards the different substitution at the 4 position. A similar result has been obtained by Rillema *et al.* for tris chelates of ruthenium(II) with bipyridine, bipyrimidine and bipyrazine.[26] The ruthenium–bibenzimidazole distances are longer than the ruthenium–bipyridine distances and proved to be invariant to changes of the degree of protonation of the bibenzimidazole. They are, however, elongated in the dinuclear complexes with respect to the mononuclear complexes (Table 1).

Mononuclear complexes 1–4 and their supramolecular aspects. In the solid state all these mononuclear complexes are accompanied by water and solvent molecules in the asymmetric unit. We could not however find any interaction between solvent molecules like acetone or acetonitrile with the complex cation. $[Ru(H_2bibzim)(dmbpy)_2][PF_6]_2\cdot 2H_2O$ **2** was formed by slow crystallisation from an acetone–water solution. The $Ru–N_{dmbpy}$ distances are somewhat longer than in $[Ru(H_2bibzim)(tbbpy)_2]^{2+}$ **3**[12] (Table 1) and are within experimental errors the same as for the $[\{Ru(dmbpy)_2\}_2(bpym)]^{4+}$ (bpym = 2,2′-bipyrimidine) system.[3] The bibenzimidazole ligand in **2** is slightly bent around the ruthenium centre. This is reflected in the angle of 166.6° resulting from two lines constructed from the centroid of the benzene ring of one half of the ligand and the corresponding bridging carbon atom. Both benzimidazole rings exhibit a slight torsion angle towards each other of 4.3°. Both N–H functions of the bibenzimidazole ligand serve as hydrogen bond donors for water molecules resulting in a nitrogen–oxygen distance of 2.811(5) Å. One water molecule which is spatially fixed by the N–H hydrogen bond forms a hydrogen bond to the neighbouring molecule (O···O distance 2.762(5) Å) which is also fixed by a N–H hydrogen bond from the same complex, see Fig. 1. The next water molecule forms a hydrogen bond to a neighbouring water molecule which is in turn hydrogen bonded by a N–H function (O···O distance 2.778(5) Å) of another molecule of **2**. The next $[Ru(H_2bibzim)(dmbpy)_2]^{2+}$ of the same strand is 3.976 Å above the plane formed by the bibenzimidazole ligand of the first complex and its hydrogen bonded water.

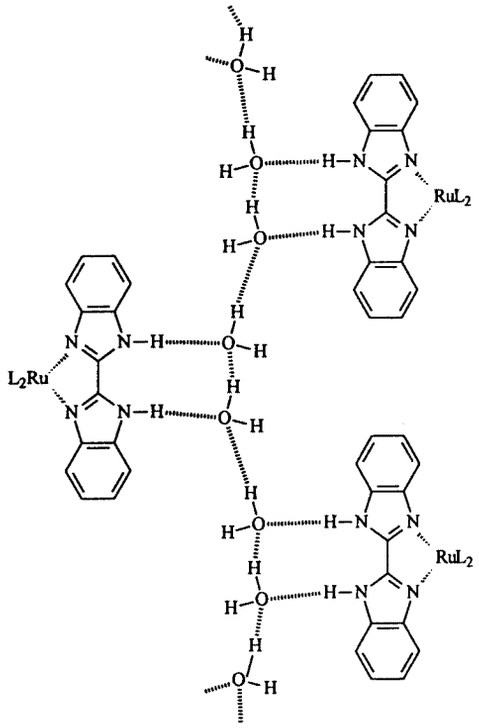

Fig. 2 Graphical representation of the supramolecular arrangement of complex **2** in the solid state; anions and acetone molecules are omitted for clarity.

This structural principle continues throughout the whole crystal and directs this highly ordered spatial orientation in such a way that the Δ enantiomer and the Λ enantiomer form separated strings which are interconnected by a one dimensional chain of water molecules (Fig. 2) and the complexes together with the water molecules are arranged in a step like manner. There are only a few examples in the literature where single molecules are interconnected by one dimensional chains of water[27] none of them being a ruthenium polypyridyl complex; even so there are a few ruthenium complexes displaying more complicated hydrogen bond networks involving water.[28] Crystal structures of ruthenium polypyridyl complexes containing the benzimidazole fragment display limited hydrogen bonding patterns.[13] If nuclear base substituted bipyridine ligands are employed structurally highly organized architectures can be obtained by suitable interaction of the heterocyclic moieties.[29]

In contrast to complex **2** the closely related $[Ru(H_2bibzim)(bpy)_2][CF_3SO_3]_2\cdot 3H_2O$ **1**, shows a completely different hydrogen bonding network (Fig. 3). Similarly to **2**, both of the protonated secondary amine functions of the bibenzimidazole are within hydrogen bonding distance to one water respectively. In contrast to the former, both water molecules are not within hydrogen bonding distance towards each other. They are however both in hydrogen bonding distance to a third water molecule and to an oxygen from a triflate counter ion ($CF_3SO_3^-$) respectively. The third water molecule is in hydrogen bonding distance to the oxygens from two different triflate counter ions. One ruthenium complex unit is therefore incorporated in a hydrogen bonding network involving three water and four triflate molecules. These triflates are also in hydrogen bonding distance to other water molecules which are in hydrogen bonding distance to another molecule of **1**. The complexes are therefore, *via* their N–H functions, interconnected by a complicated network involving (i) water molecules serving as hydrogen bond

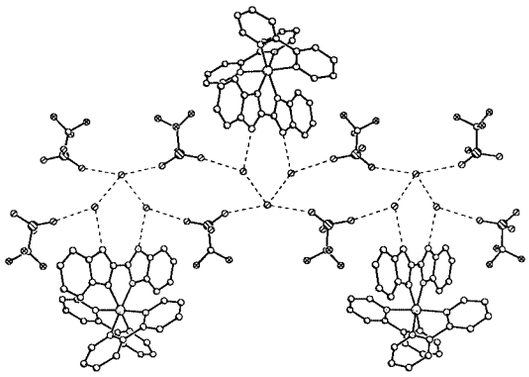

Fig. 3 Hydrogen bonding network of $[Ru(H_2bibzim)(bpy)_2][CF_3SO_3]_2 \cdot 3H_2O$ **1** in the solid state; protons and acetone molecules are omitted for clarity.

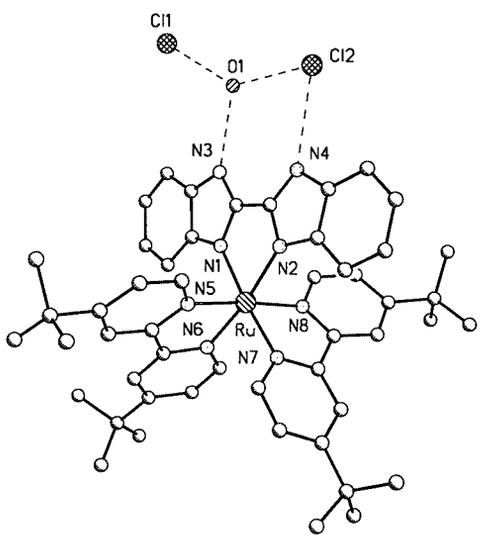

Fig. 4 Hydrogen bonding system of $[Ru(H_2bibzim)(tbbpy)_2]Cl_2 \cdot H_2O$ **3** in the solid state; protons and acetonitrile molecules are omitted for clarity.

acceptors for N–H and O–H donors and (ii) triflate molecules serving as hydrogen bond acceptors for O–H hydrogen bond donors from water molecules connected to different ruthenium complexes.

Changing the counter ion from hexafluorophosphate to triflate clearly influences the degree of spatial orientation and order. Additionally, chloride represents a suitable counter ion which is, in copper complexes of bibenzimidazole,[30] known to interact directly with the N–H function of the bibenzimidazole. A ruthenium bibenzimidazole complex would therefore have the opportunity to interact either with water or chloride ions.

In a recent communication[12] we reported internal structural parameters of $[Ru(H_2bibzim)(tbbpy)_2]Cl_2 \cdot H_2O$ **3**. In order to compare the supramolecular aspects of **3** with those of **1** and **2** we discuss here the hydrogen bonding network displayed by **3**. In the solid state both N–H functions are protonated and act as hydrogen bond donors (Fig. 4). In contrast to the previous two structures of **1** and **2** one hydrogen bond is formed to a counter ion Cl^- ($N \cdots Cl^-$ 3.080(4) Å), the second to a molecule of water which is displaced over two positions and the discussion will use the weighted position ($N \cdots O$ 2.626(4) Å). The water serves as hydrogen bond donor to the N–H bonded Cl^- ($O \cdots Cl^-$ 3.039(4) Å) and to the second Cl^- with an oxygen–chloride distance of 3.022(4) Å. Even so the bibenzimidazole ligand does serve as a hydrogen bond donor; similar to the former systems, no further supramolecular aggregation could be observed.

When we go from the bibenzimidazole **1**–**3** to the bibenzimidazolate complexes the question arises as to how the transformation of the secondary amine functions to amide functions influences the hydrogen bonding network. If [Ru(bibzim)-(tbbpy)$_2$] **4** is crystallized from neat acetonitrile no supramolecular assemblies can be observed.[12] However when the same complex is crystallized from an acetone–water mixture two molecules of water are 2.819(5) Å, within hydrogen bonding distance, to the nitrogens of the deprotonated bibenzimidazole ligand and 3.036(5) Å towards each other as well (Fig. 5). This hydrogen bonding interaction does not seem to affect internal structural parameters of the ruthenium complex.

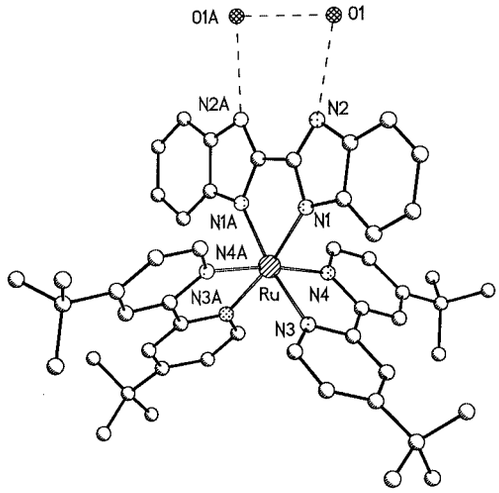

Fig. 5 Hydrogen bonding network of $[Ru(bibzim)(tbbpy)_2] \cdot 2H_2O$ **4**, protons and acetone molecules are omitted for clarity.

It seems reasonable to assume that the water molecules serve as hydrogen bond donors towards the negatively polarized bibenzimidazole nitrogens. Additionally one molecule of water serves as hydrogen bond donor for the second water molecule. This system could, in principle, form aggregates similar to **1** and **2**. However, the transformation of the bibenzimidazole unit from a hydrogen-bond donor to an acceptor seems to prevent similar supramolecular arrangements. Even so the degree of protonation does not seem to affect internal structural parameters although it does strongly influence the supramolecular structure of the mentioned complexes.

Binuclear complexes. Deprotenation of the bibenzimidazole ligand turns the corresponding complex into a very reactive metallo ligand.[12] The combination of two octahedral complex fragments in one molecule ultimately leads to three diastereomeric isomers the *meso* form ΔΛ and the ΔΔ, ΛΛ isomers whose racemic mixture is referred to as *rac*. The problem stays at a relatively simple level if symmetric bridging ligands are employed. *meso*-[{Ru(tbbpy)$_2$}$_2$(bibzim)][PF$_6$]$_2$ **5a** and *meso*-[{Ru(bpy)$_2$}$_2$(bibzim)][PF$_6$]$_2$ **6** belong to this group.

The *tert*-butyl substituted homodinuclear complex **5a** could be crystallized from a solution of a purified fraction by slow evaporation of the solvent. Its molecular structure is depicted in Fig. 6. The $Ru–N_{tbbpy}$ distances of 2.040(3) to 2.065(3) Å are not significantly different from those in the related mononuclear complexes described above and correlate well with values reported for the related biimidazolate (biim) complex.[6] The $Ru–N_{bibzim}$ distances are at 2.164(3) Å significantly longer than in the investigated mononuclear complexes.

The homodinuclear complex *meso*-[{Ru(bpy)$_2$}$_2$(bibzim)]-[PF$_6$]$_2$ **6** could be crystallized from a mixture of the diastereomeric isomers by slow evaporation of an acetonitrile solution. The $Ru–N_{bpy}$ distances of 2.021(4) to 2.043(4) Å are not significantly different from the related mononuclear complexes described above and correlate well with the values recently reported for *meso*-[{Ru(bpy)$_2$}$_2$(biim)][ClO$_4$]$_2$.[6] The $Ru–N_{bibzim}$ distances are, however, at 2.139(4) Å significantly longer than in the investigated mononuclear complexes[12] but correlate well

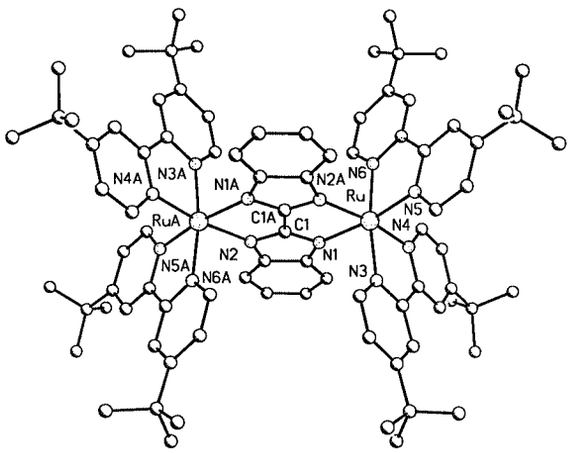

Fig. 6 Structure of *meso*-[{Ru(tbbpy)$_2$}$_2$(bibzim)][PF$_6$]$_2$ **5a**; protons, anions and solvent molecules are omitted for clarity.

with the values reported for the dinuclear biimidazolate complex. They also seem to be slightly shorter compared to those of **5a**. The bibenzimidazole ligand in both dinuclear complexes is not bent around a single ruthenium and no torsion angle between the benzimidazole moieties could be observed.

The structural evidence implies that upon going from the mononuclear to the dinuclear complexes a weakening of the bonding interaction between the ruthenium(II) centre and the bridging bibenzimidazole occurs. If bibenzimidazole is acting as a bridging ligand it is double deprotonated and turns into a much stronger σ donor.[7] The increased σ donor strength might cause a decrease of the acceptor abilities. However since the ruthenium–bibenzimidazole distances in the mononuclear deprotonated complex **4**[12] are much shorter than in the dinuclear complexes differences in the ligand properties cannot fully explain the differences in bond lengths for the mono- and di-nuclear complexes observed in the structural data obtained from X-ray investigations. Comparing the data obtained it is evident that substitution at the 4 position of the peripheral bipyridine system has no significant influence on structural parameters of the ruthenium complexes (see Table 1).

NMR spectroscopy of complexes 1–3 and 5

NMR spectroscopy has proved to be a useful tool in the structural characterization of ruthenium polypyridyl complexes[31] but with a few exceptions[32] has not been used to any great extent in the structural characterization of polypyridyl ruthenium bibenzimidazole complexes. The protonated mononuclear complexes [Ru(H$_2$bibzim)(bpy)$_2$]$^{2+}$ **1**, [Ru(H$_2$bibzim)(dmbpy)$_2$]$^{2+}$ **2** and [Ru(H$_2$bibzim)(tbbpy)$_2$]$^{2+}$ **3** exhibit C_2 symmetry in solution. The protons of the secondary amine function of the bibenzimidazole ligand are not detectable in CD_2Cl_2, DMSO, acetone or acetonitrile and a direct investigation into its involvement in hydrogen bonding was therefore precluded. While the chemical shifts of the aromatic bibenzimidazole protons are almost unaffected by either different substitution or solvent (Table 2), the bipyridine based protons exhibit a large shift on changing the deuteriated solvents from acetone to acetonitrile. It is very unlikely that these shifts are due to interaction of the secondary amine protons of bibenzimidazole with solvent molecules since similar shifts have been observed for [Ru(tbbpy)$_3$]$^{2+}$ (Table 2).

The NMR spectra of the diastereomeric forms of complex **5** are different (Fig. 7). The signals for one pyridine system remain relatively unchanged in both forms, however, the positions of the H5b and H6b protons of the other pyridine moiety are considerably shifted upfield in the spectrum of the *rac* fraction if compared with that of the *meso* form (Table 2). This is consistent with results obtained for the strongly related [{Ru(dmbpy)$_2$}$_2$(bpym)]$^{4+}$ system[3] and has been explained in terms

Table 1 Selected bond lengths (Å) and angles (°) of [Ru(H$_2$bibzim)(bpy)$_2$][CF$_3$SO$_3$]$_2$ **1**, [Ru(H$_2$bibzim)(dmbpy)$_2$][PF$_6$]$_2$ **2**, [Ru(H$_2$bibzim)(tbbpy)$_2$]Cl$_2$ **3**,[12] [Ru(bibzim)(tbbpy)$_2$]·2H$_2$O **4**, *meso*-[{Ru(tbbpy)$_2$}$_2$(bibzim)][PF$_6$]$_2$ **5a** and *meso*-[{Ru(bpy)$_2$}$_2$(bibzim)][PF$_6$]$_2$ **6**

	1	**2**	**3**	**4**	**5a**	**6**
Ru–N(bpy)	2.046(6)–2.066(6)	2.045(3)–2.051(3)	2.024(2)–2.058(2)	2.055(4)–2.056(4)	2.040(3)–2.065(3)	2.021(4)–2.043(4)
Ru–N(bibzim)	2.100(6)–2.101(6)	2.088(3)	2.094(2)–2.097(2)	2.099(4)	2.160(3)–2.164(3)	2.135(4)–2.139(4)
N(bpy)–Ru–N(bpy)	78.6(2)	78.66(11)	78.08(9)–78.26(9)	78.95(14)	78.81(13)–78.87(13)	79.0(2)–79.1(2)
N(bibzim)–Ru–N(bibzim)	77.4(3)	77.3(2)	77.14(9)	77.0(2)	80.89(12)	81.3(2)
Bending angle of bibzim	166.1	166.6	166.3	169.3	180	180
Torsion angle of bibzim	4.5	4.3	3.8	1.2	1.3	0.4
N–C–N angle of bibzim	113.0(5)	112.3(3)	113.2(3)	116.8(5)	117.9(3)	118.0(4)

Table 2 ^{1}H NMR data of complexes **1**–**3**, **5** and $[Ru(tbbpy)_3][PF_6]_2$ **A** in acetone-d_6 and acetonitrile-d_3

	Chemical shifts in acetone-d_6						Chemical shifts in acetonitrile-d_3			
Proton	**1**	**2**	**3**	**5a**	**5b**	**A**	**1**	**2**	**3**	**A**
H3a	8.84	8.57	8.83	8.76	8.76	8.86	8.52	8.37	8.51	8.46
H3b	8.80	8.46	8.72	8.68	8.73		8.43	8.28	8.42	
H6a	8.27	7.94	7.96	8.16	8.09	7.82	7.97	7.80	7.87	7.55
H6b	8.16	7.80	8.02	8.32	7.78		7.97	7.71	7.76	
H5b	8.05	7.18	7.61	7.70	7.29		7.38	7.11	7.35	
H3BL	7.82	7.80	7.80	6.66/5.66[a]	6.66/5.66[a]		7.78	7.71	7.76	
H5a	7.62	7.38	7.43	7.56	7.51	7.57	7.38	7.27	7.48	7.39
H4BL	7.44	7.38	7.38	6.66/5.66[a]	6.66/5.66[a]		7.38	7.37	7.43	
H5BL	7.08	7.02	7.02	6.66/5.66[a]	6.66/5.66[a]		7.05	7.03	7.06	
H6BL	5.87	5.86	5.78	6.66/5.66[a]	6.66/5.66[a]		5.76	5.83	5.68	
4 position	8.27 H4a	2.57 CH_3a	1.47 C_4H_9	1.43 C_4H_9	1.43 C_4H_9	1.38 C_4H_9	8.11 H4a	2.57 CH_3a	1.47 C_4H_9	1.39 C_4H_9
4 position	7.44 H4b	2.41 CH_3b	1.33 C_4H_9	1.34 C_4H_9	1.38 C_4H_9		7.97 H4b	2.42 CH_3b	1.35 C_4H_9	

[a] Owing to multiple peak overlap no assignment is possible.

Table 3 Photo- and electro-chemical data in acetonitrile of complexes **1**–**6**

	λ_{max}/nm				
Complex	absorption	emission	Lifetime/ns	E_{ox}/V	E_{red}/V
1	463[a]	640[a]	131[b]	1.12[a]	−1.53/−1.86[b]
2	465	650	90	0.99	
3	473	648	120	0.99	*ca.* −0.7 to −1.2
4	580	—	—	0.39	−1.16/−1.25
5a	510	700	50	0.64/0.95	−1.07/−1.21
5b	510	700	60	0.64/0.95	−1.07/−1.21
6	505	695	60[b]	0.76/1.04[a]	−1.49/−1.78[b]

[a] Ref. 7. [b] Ref. 9.

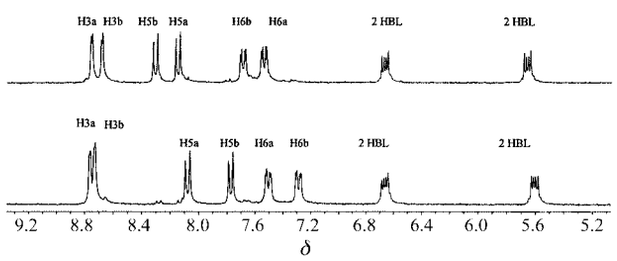

Fig. 7 ^{1}H NMR spectra of the *meso* (top) (**5a**) and *rac* (bottom) (**5b**) forms of $[\{Ru(tbbpy)_2\}_2(bibzim)][PF_6]_2$ in acetone-d_6.

of a greater anisotropic effect from the ring current of the adjacent bipyridine system experienced by H5b and H6b protons which are directly over the bridging ligand. The NMR spectrum of the first fraction was assigned to the *meso* form since crystals suitable for X-ray diffraction could be obtained from the purified fraction.

Photophysical and electrochemical properties of complexes 1–6

Alkyl substituents at bipyridine ligands should have an inductively electron donating effect on the aromatic system of the corresponding pyridine ring. In order to investigate the influence of substitution on the properties of the ruthenium complexes the oxidation potentials were determined. Alkyl substitution at the 4 position of the bipyridine ligand leads to a roughly 0.1 V shift towards lower oxidation potential of all mono- and di-nuclear complexes investigated which is in agreement with results obtained for $[\{Ru(dmbpy)_2\}_2(bibzim)][ClO_4]_2$ [33] (Table 3). These results suggest that substitution with aliphatic groups has an influence on the electronic situation at the central metal atom. It seems likely that the +I effect of the alkyl substituent results in an increase of the electron density at the metal.

As expected, deprotonation of the bibenzimidazole ligand leads to a large shift of 0.6 V towards more negative potentials for the oxidation of the ruthenium centre. This indicates an enhanced electron density at the metal centre induced by the deprotonation.

Substitution also influences the reduction properties which are related to the bipyridine system.[5] The most pronounced effect can be attributed to deprotonation of the bibenzimidazole ligand. The not well resolved reduction of the protonated complex is replaced by a two step wave for the deprotonated complex. However due to the complexity of the data obtained for the protonated complex no direct comparison of reduction potentials is possible. Haga investigated the non-substituted complex and did not find a large shift in reduction potentials for the protonated and deprotonated form.[7]

Owing to the intrinsic nature of the MLCT process an increase of the electron density at the ruthenium centre should also influence the photophysical properties of the complex. However, the absorption and emission properties of the complexes (Table 3) do not support this assumption. The mononuclear unsubstituted ruthenium complex **1** absorbs in the visible range at 463 nm. The emission is at 640 nm.[7,9] Whilst the absorption maxima of the series **1** to **3** do show a slight bathochromic shift, the wavelength of emission seems not to be affected at all (Table 3). An investigation of the lifetime of the excited state shows that all three mononuclear complexes have quite similar lifetimes (Table 3). An acetonitrile solution of the dried protonated complex **3** showed no differences to the above described values for absorption maximum and emission wavelength. However, if the same complex is dissolved in water a small bathochromic shift in the absorption maximum is observed and a bathochromic shift of 30 nm in the emission wavelength as well. A similar experiment with $[Ru(tbbpy)_3]^{2+}$ showed that the UV-vis spectrum and the wavelength of emission are nearly invariant changing from acetonitrile to water. Comparison indicates that different environments at the N–H functions in solution influence photophysical properties and that water also serves as a hydrogen bond acceptor in

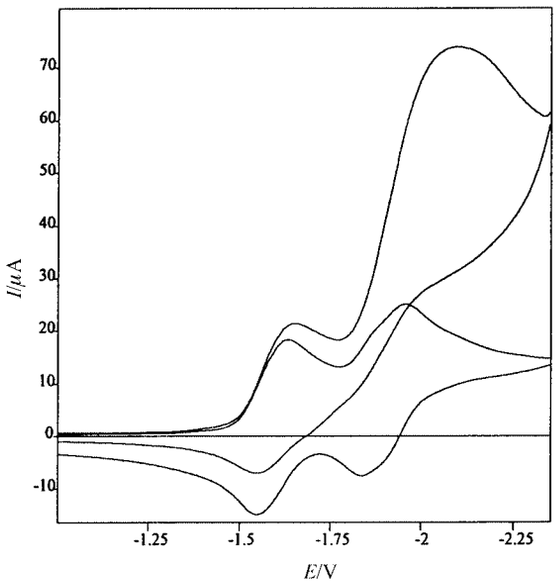

Fig. 8 Negative cyclic voltammogram of $[\{Ru(tbbpy)_2\}_2(bibzim)][PF_6]_2$ **5a/5b** in acetonitrile *vs.* SCE; (lower) two one electron reductions under an argon atmosphere; (upper) catalytic current enhancement under a CO_2 atmosphere.

solution whereas acetonitrile does not interact to a great extent with the N–N functions.

As discussed earlier,[12] deprotonation of the bibenzimidazole forming **4** results in a loss of emission and bathochromic shift of the absorption maxima.

Both dinuclear *tert*-butyl substituted stereoisomers **5a/5b** absorb at 510 nm in the visible range and emit at 700 nm. Complex **6** absorbs at 505 nm and we determined the emission wavelength at 695 nm. Substitution of the pyridine ligand does not seem to influence photophysical properties to a great extent.

Most intriguing was the investigation into the lifetime of the excited state of the two sets of stereoisomers **5a/5b**. The lifetimes of the lowest excited states of both the *meso* and the *rac* isomer were 60 ± 2 ns. The apparent absence of any influence of the stereochemistry on the lifetime of the lowest excited states in dinuclear bibenzimidazole complexes is in contrast to the observations made for stereoisomers of dinuclear HAT (hexaazatriphenylene) based systems.[16] However in the latter emission occurs from the triplet MLCT ruthenium HAT state.[34] In the case of the dinuclear bibenzimidazole complexes the ancillary bipyridines[7] act as the luminophore. This might be a tentative explanation for the observed independence of the lifetime of the lowest excited state of the stereochemistry at the ruthenium. Comparison with literature values of excited state lifetimes obtained for the unsubstituted isomer **6**, of 60 ns[9] shows that also in the dinuclear complexes the substitution with *tert*-butyl groups has no pronounced influence on the excited state lifetime.

Electrochemical CO_2 reduction

Complexes **3**, **4** and a racemic mixture of **5a** and **5b** were investigated for their activity in electrochemical carbon dioxide reduction. Some ruthenium polypyridyl systems[35] exhibit a remarkable activity and selectivity in this process whereas others do not show any activity.[10] Since deprotonation of the bibenzimidazole ligand enhances its σ-donor properties an influence on the electrochemical reactivity can be envisaged.

All investigated complexes can be reduced and at least two reversible one electron reduction processes can be discerned whereas the protonated complex exhibits a much more complex behaviour. In the presence of CO_2 an increase in the cathodic current can be observed for both steps (Fig. 8) for all three compounds. The increase is relatively small for the first reduction step whereas a relatively strong increase for the second step can be observed. This indicates that the two electron reduced species is the most active catalyst which transforms the carbon dioxide. The degree of increase of the current is dependent on the complex. The protonated complex **3** exhibits only a relatively small increase in current. The deprotonated complex **4** is roughly twice as active judging from the current enhancement and the dinuclear complex **5a/5b** is even more active than the deprotonated mononuclear complex.

Preliminary investigation into the range of products obtained during an exhaustive reduction of carbon dioxide in a CO_2 saturated 0.1 M acetonitrile solution of these complexes using **3** showed the production of carbon monoxide (1–2%) and oxalate (*ca.* 10%). If, however, the deprotonated complex **4** was employed oxalate was produced with 43% current efficiency beside some carbon monoxide (1–2%). The course of the reaction was monitored using UV-vis spectroscopy. The protonated complex showed in the initial phase a sharp decrease in the absorption and a shift in the maxima from 473 to 548 nm. This new band continued to decrease during the electrolysis and disappeared completely. For the deprotonated complex no such shifts could be observed however the absorption decreased. This result suggests that some electrical energy is consumed by transformation of the protonated complex. This significant relation between structure and reactivity even for the two mononuclear complexes together with their known interaction with water which might alter the range of products obtained[10] will be investigated in more detail.

Conclusion

This work represents to the best of our knowledge the first crystallographic investigation into supramolecular aspects of ruthenium bibenzimidazole complexes. The assembly of highly spatially ordered arrays of mononuclear ruthenium bibenzimidazole complexes is possible for **2** by exploiting the hydrogen bond donor activity of bibenzimidazole towards water. It could also be shown that the choice of counter ions influences the supramolecular structure in the solid state. The nature of the hydrogen bonding activity of ruthenium bibenzimidazole complexes can be reversed from donor to acceptor by deprotonation of the secondary amine which has only a small influence on internal structural parameters. However the resulting species although in principle capable of forming polymeric supramolecular structures bridged by water molecules remains isolated. The deprotonated complex **4** represents a reactive metallo ligand.[12]

By using two dimensional NMR it was also possible to show that two diastereomeric forms of the homodinuclear complexes exist (**5a/5b**) and can be separated. The lifetime of the lowest excited state proved to be independent of the stereochemistry at the ruthenium.

Alkyl substitution at the 4 position of the corresponding pyridine unit resulted in a negative shift of the oxidation potential of the ruthenium. It is possible to switch off the emission of complex **3** by deprotonation of the secondary amine function of the bibenzimidazole ligand.[12]

The mononuclear protonated complex **3**, its deprotonated analogue **4** and the dinuclear complex **5a/5b** are active catalysts in electrochemical carbon dioxide reduction. The reactivity and selectivity of the mononuclear complexes depends on the degree of protonation since **4** exhibits a nearly twofold enhancement of the catalytic current and a 300% increase in current efficiency in oxalate production if compared with that of **3**.

Acknowledgements

S. R. and M. R. acknowledge the "Studienstiftung des

Deutschen Volkes" for a Ph.D. grant. Financial support from the Deutsch Forschungsgemeinschaft (SFB 436) is gratefully acknowledged. M. D., C. O'C. and J. G. V. thank the EC TMR programme (grants number CT96-0031 and CT96-0076) for financial assistance.

References

1 V. Balzani, A. Juris, M. Venturi, S. Campagna and S. Serroni, *Chem. Rev.*, 1996, **96**, 759; J. P. Sauvage, J. P. Collin, J. P. Chambron, S. Guillerez, C. Coudret, V. Balzani, F. Barigelletti, L. De Cola and L. Flamingi, *Chem. Rev.*, 1994, **94**, 993.
2 V. Balzani and F. Scandola, *Supramolecular Photochemistry*, Ellis Horwood, Chichester, 1991; L. Sun, H. Berglund, R. Davydov, T. Norrby, L. Hammarström, P. Korall, A. Börje, C. Philouze, K. Berg, A. Tran, M. Andersson, G. Stenhagen, J. Mårtensson, M. Almgren, S. Styring and B. Åkermark, *J. Am. Chem. Soc.*, 1997, **119**, 6996; G. S. Hanan, C. R. Arana, J. M. Lehn and D. Fenske, *Angew. Chem.*, *Int. Ed. Engl.*, 1995, **34**, 1122; F. Barigelletti, L. Flamingi, V. Balzani, J. P. Collin, J. P. Sauvage, A. Sour, E. C. Constable and A. M. W. Cargill Thompson, *J. Am. Chem. Soc.*, 1994, **116**, 7692; A. Harriman and R. Ziessel, *Chem. Commun.*, 1996, 1707; F. Barigelletti, L. Flamingi, J. P. Collin and J. P. Sauvage, *Chem. Commun.*, 1997, 333.
3 N. C. Fletcher, P. C. Junk, D. A. Reitsma and F. R. Keene, *J. Chem. Soc.*, *Dalton Trans.*, 1998, 133.
4 S. Serroni, G. Denti, S. Campagna, A. Juris, M. Ciano and V. Balzani, *Angew. Chem.*, *Int. Ed. Engl.*, 1992, **31**, 1493.
5 A. J. Downard, G. E. Honey, L. F. Phillips and P. J. Steel, *Inorg. Chem.*, 1991, **30**, 2259.
6 P. Majumadra, S. Peng and S. Goswami, *J. Chem. Soc.*, *Dalton Trans.*, 1998, 1569.
7 M. Haga, *Inorg. Chim. Acta*, 1980, **45**, L183; M. Haga, *Inorg. Chim. Acta*, 1983, **75**, 29; M. Haga, T. Matsumura-Inoue and S. Yamabe, *Inorg. Chem.*, 1987, **26**, 4148.
8 M. Haga and A. Tsunemitsu, *Inorg. Chim. Acta*, 1989, **164**, 137.
9 D. P. Rillema, R. Sahai, P. Matthews, A. K. Edwards, R. J. Shaver and L. Morgan, *Inorg. Chem.*, 1990, **29**, 167.
10 Md. M. Ali, H. Sato, T. Mizukawa, K. Tsuge, M. Haga and K. Tanaka, *Chem. Commun.*, 1998, 249.
11 M. Haga, Md. M. Ali and R. Arakawa, *Angew. Chem.*, *Int. Ed. Engl.*, 1996, **35**, 76.
12 S. Rau, T. Büttner, C. Temme, M. Ruben, H. Görls, D. Walther, M. Duati, S. Fanni and J. G. Vos, *Inorg. Chem.*, 2000, **39**, 1621; for other ruthenium polypyridyl based sensors see A. P. de Silva, H. Q. N. Gunaratne, T. Gunnlaugsson, A. J. M. Huxley, C. P. McCoy, J. T. Rademacher and T. E. Rice, *Chem. Rev.*, 1997, **97**, 1515; F. Barigelletti, L. Flamingi, G. Calogero, L. Hammerström, J.-P. Sauvage and J. P. Collin, *Chem. Commun.*, 1998, 2333.
13 M. Haga, M. M. Ali, S. Koseki, K. Fujimoto, A. Yoshimura, K. Nozaki, T. Ohno, K. Nakajima and D. J. Stufkens, *Inorg. Chem.*, 1996, **35**, 3335; D. Carmona, J. Ferrer, A. Mendoza, F. J. Lahoz, L. A. Oro, F. Viguri and J. Reyes, *Organometallics*, 1995, **14**, 2066; S. Baitalik, U. Flörke and K. Nag, *Inorg. Chem.*, 1999, **38**, 3296.
14 M. J. Uddin, A. Yoshimura and T. Ohno, *Bull. Chem. Soc. Jpn.*, 1999, **72**, 989.
15 S. S. Turner, C. Michaut, O. Kahn, L. Quahab, A. Lecas and E. Amouyal, *New J. Chem.*, 1995, **19**, 773; N. W. Alcock, P. R. Barker, J. M. Haider, M. J. Hannon, C. L. Painting, Z. Pikramenou, E. A. Plummer, K. Rissanen and P. Saarenketo, *J. Chem. Soc.*, *Dalton Trans.*, 2000, 1447.
16 T. J. Rutherford, O. Van Gitje, A. Kirsch-De Mesmaeker and F. R. Keene, *Inorg. Chem.*, 1997, **36**, 4465; U. Knopf and A. v. Zelewsky, *Angew. Chem.*, *Int. Ed.*, 1999, **38**, 302.
17 M. A. Bennett and G. Wilkinson, *Chem. Ind.*, 1959, 1516.
18 E. S. Lane, *J. Chem. Soc.*, 1955, 1079.
19 T. B. Hadda and H. Le Bozec, *Polyhedron*, 1988, **7**, 575.
20 B. P. Sullivan, D. J. Salmon and T. J. Meyer, *Inorg. Chem.*, 1978, **17**, 3334.
21 T. Togano, N. Nagano, M. Tsuchida, H. Kumakura, K. Hisamatsu, F. S. Howell and M. Mukaida, *Inorg. Chim. Acta*, 1992, **195**, 221.
22 *Gmelin Handbuch*, Erweiterungswerk for the 8th edition, Springer, Berlin–New York, 1974, B 14, A 1, ch. 2.4, pp. 80–89.
23 Z. Otwinowski and W. Minor, *Methods Enzymol.*, 1997, **276**.
24 G. M. Sheldrick, *Acta Crystallogr.*, *Sect. A*, 1990, **46**, 467.
25 G. M. Sheldrick, SHELXL 97, University of Göttingen, 1997.
26 D. P. Rillema, D. S. Jones, C. Woods and H. A. Levy, *Inorg. Chem.*, 1992, **31**, 2935.
27 Thanks to Dr. Greg Shields, CCDC, for helping with the search for one dimensional water chains; J. P. Glusker, H. L. Carrell, H. M. Berman, B. Gallen and R. M. Peck, *J. Am. Chem. Soc.*, 1977, **99**, 595; R. Kaplonek, G. Fechtel, U. Baumeister and H. Hartung, *Z. Anorg. Allg. Chem.*, 1992, **617**, 161; E. Psillakis, J. C. Jeffery, J. A. McCleverty and M. D. Ward, *J. Chem. Soc.*, *Dalton Trans.*, 1997, 1645.
28 M. Ruben, S. Rau, A. Skirl, K. Krause, D. Walther and J. G. Vos, *Inorg. Chim. Acta*, 2000, **303**, 206; C. Anderson and A. L. Beauchamp, *Inorg. Chem.*, 1995, **34**, 6065; C. Sudha, S. K. Mandal and A. R. Chakravarty, *Inorg. Chem.*, 1998, **37**, 270.
29 C. M. White, M. F. Gonzalez, D. A. Bardwell, L. H. Rees, J. C. Jeffery, M. D. Ward, N. Armaroli, G. Calogero and F. Barigelletti, *J. Chem. Soc.*, *Dalton Trans.*, 1997, 727.
30 S. de Souza Lemos, K. E. Bessler and E. Schulz Lang, *Z. Anorg. Allg. Chem.*, 1998, **624**, 701.
31 A. C. Lees, B. Evrard, T. E. Keyes, J. G. Vos, C. J. Kleverlaan, M. Alebbi and C. A. Bignozzi, *Eur. J. Inorg. Chem.*, 1999, 2309.
32 M. Haga, *Inorg. Chim. Acta*, 1983, **77**, L39.
33 M. Haga and A. M. Bond, *Inorg. Chem.*, 1991, **30**, 475.
34 A. Kirsch-De Mesmaeker, L. Jacquet, A. Masschelein, F. Vanhecke and K. Heremans, *Inorg. Chem.*, 1989, **28**, 2465.
35 F. R. Keene and B. P. Sullivan, in *Electrochemical and Electrocatalytical Reactions of Carbon Dioxide*, eds. B. P. Sullivan K. Kirst and H. E. Guard, Elsevier, Amsterdam, 1993, ch. 5, pp. 118–144 and references cited therein.